Indian Journal of Experimental Biology
Vol. 63, October 2025, pp. 844-856
DOI: 10.56042/ijeb.v63i10.15874

Investigating anticancer potential of methanolic extract of *Cyperus rotundus* rhizome: *In vitro* analysis on Dalton′s lymphoma cells and toxicity evaluation in mouse model

Abhinandan Choudhury, Namram Sushindrajit Singh & Akalesh Kumar Verma*
Department of Zoology, Cotton University, Guwahati 781001, India

Received 29 December 2024; revised 14 July 2025

Cyperus rotundus Linn (CR), commonly known as nutgrass or purple nutsedge has long been valued in traditional medicine for its diverse pharmacological properties, including anti-inflammatory, antimicrobial, antioxidant and anticancer activities. The anticancer activity of CR methanolic extract was investigated using Dalton′s lymphoma (DL) cells, while its toxicity profile was evaluated in normal mice to assess safety *in vivo*. The rhizomes were extracted using 70% methanol and subjected to phytochemical screening revealing a diverse range of bioactive compounds including carbohydrates, proteins, amino acids, lipids and other active substances. High performance thin layer chromatography (HPTLC) was further performed on the CR extract to obtain its phytochemical fingerprint. *In vitro* cytotoxicity assays demonstrated that a single dose (200 µg/mL) of CR extract induced significant time-dependent cytotoxicity in DL cells as evidenced by the Trypan Blue exclusion assay and eosin staining method. Morphological observations revealed apoptotic features such as membrane blebbing and vacuolarization confirming apoptosis induction. Histopathological analysis of heart, lungs, liver, spleen, kidneys, testes and ovary following a single high-dose (5000 mg/kg b.w.) administration of the extract revealed no significant histological alterations. The preserved tissue architecture across all examined organs suggests that the extract is well-tolerated and does not elicit overt toxicity at this dosage, supporting its preliminary safety profile. The findings demonstrate the potential of CR rhizome extract as a natural anticancer agent with minimal toxicity. Further investigations are required to elucidate the underlying molecular mechanisms and to confirm the therapeutic efficacy of the extract in clinical settings.

Keywords: Cancer, Antitumor, Phytochemicals, Traditional medicine, Histology

Introduction

Herbal products have become increasingly significant in traditional medicine systems such as Ayurveda, Siddha, and Unani. These systems contribute valuable ethnopharmacological knowledge, offering new perspectives in medicine and supporting the development of effective treatments with minimal side effects[1,3]. Plant nutrients are utilized for extracting bioactive compounds with pharmaceutical benefits[4,5]. Among the numerous health challenges addressed by both traditional and modern medicine, cancer remains one of the most formidable. It is a leading cause of death worldwide and continues to pose a major challenge to global healthcare. The high incidence and mortality rates reflect the seriousness of the disease in both developing and developed nations[6,7]. Conventional cancer treatments including surgery, radiation, chemotherapy, immunotherapy, and angiogenesis inhibitors have had varying degrees of success, but their adverse side effects often limit their use. Despite ongoing research, the widespread clinical adoption of plant-based chemotherapeutic agents remains constrained due to insufficient large-scale studies on their safety and efficacy. Consequently, there is an ongoing need for safer and more effective anticancer compounds[8,9].

Cyperus rotundus Linn. Belonging to the family Cyperaceae, is widely recognised in traditional medicine and is known by various names such as purple nutsedge, nutgrass, motha, and musta[10]. It is particularly esteemed in Ayurveda, where it is frequently used for its effectiveness in managing gastrointestinal and joint disorders[11,12]. This herb is valued for its diverse therapeutic benefits, which have been supported by numerous studies. Research involving both animals and humans has revealed that CR exhibits several pharmacological properties, including anti-inflammatory, antidiabetic, anticoagulant, anti-arthritic, antibacterial, anticancer, anti-candida, anticonvulsant,

*Correspondence:
E-mail: akhilesh@cottonuniversity.ac.in

antihistaminic, antimalarial, anti-obesity, antipyretic, antispastic, gastroprotective, hypotensive, sedative and analgesic effects[13-16]. These findings highlight the plant's potential as a significant medicinal resource for various health conditions. The methanolic rhizome extract of the plant was also found to exhibit cytotoxic response that inhibits cell proliferation and induces apoptosis in different cancer cell lines[17]. Due to the presence of diverse bioactive compounds and its broad range of pharmacological properties, including anti-inflammatory and notable cytotoxic effects, CR holds significant therapeutic potential. With these given attributes, our present study aimed to investigate the anticancer effects of CR emphasising on its ability to inhibit cell proliferation and induce apoptosis in Dalton's lymphoma (DL) cells. These findings will offer valuable insights into the plant's anticancer properties and pave the way for further exploration of the underlying molecular mechanisms and the isolation of active compounds.

Materials and Methods

Collection and identification of plant material

The rhizomes of the CR commonly known as nutgrass were harvested from outfields of Amingaon (26.185135° N, 91.666771° E), Guwahati, Kamrup district, Assam, India in the months of October and November, 2023 (Fig. 1) and authenticated by Dr. Souravjyoti Borah, Department of Botany, Gauhati University with reference no: *Herb/GUBH/ 2023/072*, Accession No. GUBH20426 and a herbarium for the same have been deposited for further reference.

Preparation of rhizome extracts

After cleaning, shade drying and grinding the rhizome into coarse powder, the powder weighing (172.16 g) was extracted with 860 mL of 70% methanol (maintain a 1:5 w/v ratio) to ensure sufficient solvent penetration and effective extraction of phytoconstituents. The extraction procedure was optimised to ensure efficient extraction and performed three times at 24-hour intervals at room temperature (28°C). The solvent extract was filtered and concentrated by evaporating excessive solvent under reduced pressure at 40 °C using a rotary evaporator to prepare the crude extract[18]. The final yield of the crude was 14.13%.

Phytochemical detection by qualitative analysis

The crude extract was tested for the presence of carbohydrates, sugars (mono and polysaccharides),

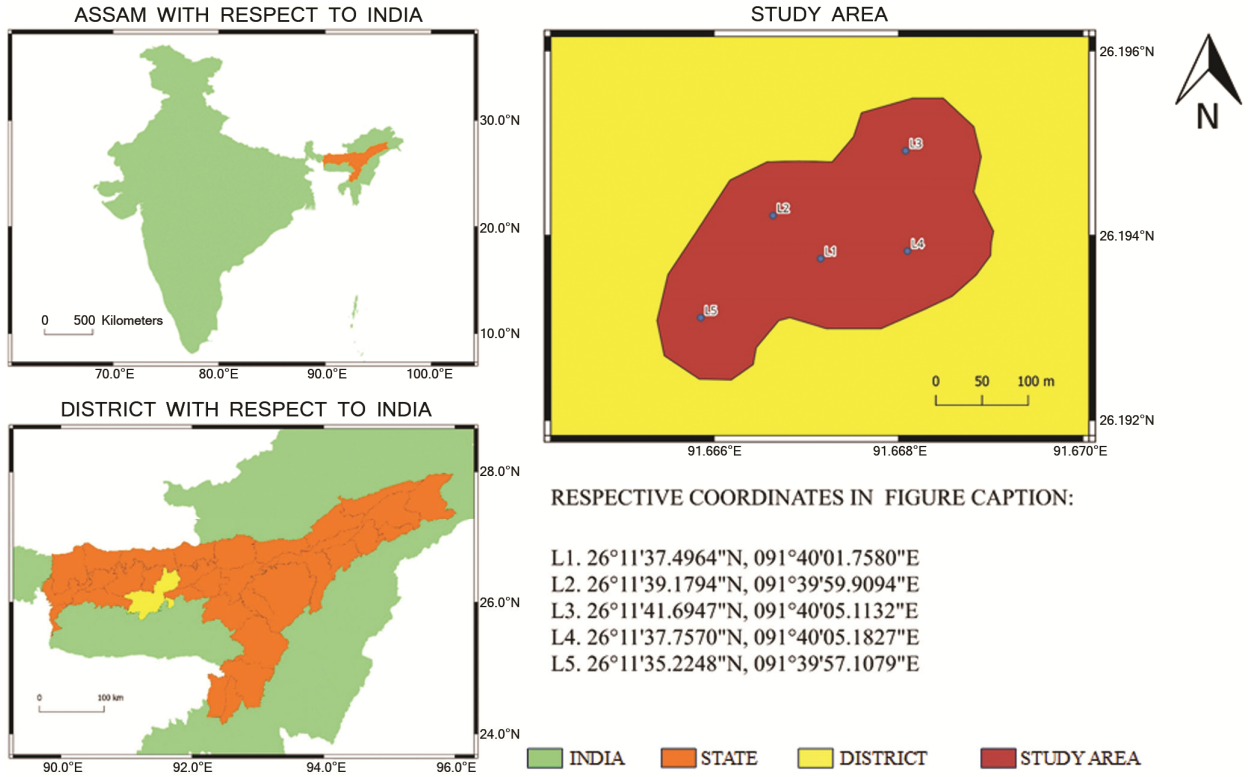

Fig. 1 — Map depicting the collection sites of rhizome samples across various locations in Amingaon, Kamrup District, Guwahati, Assam, India, along with their respective coordinates.

protein and lipids [19,20]. All tests were performed thrice. For qualitative analysis, a stock solution was prepared by dissolving 100 mg of the crude methanolic extract in 10 mL of distilled water to form a 10 mg/mL stock solution. This aqueous solution was thoroughly vortexed and filtered to remove insoluble debris. The resulting clear solution was used consistently across all qualitative phytochemical tests.

Molisch's test for carbohydrate

Total 2 mL of the sample solution (Crude extract + Distilled water), 2 drops of Molisch's reagent was added. Then 2 mL of concentrated sulphuric acid was added through the sides of the test tube. Violet coloured ring appeared at the junction of the liquids indicating the presence of carbohydrates.

Fehling's test for sugar (monosaccharides):

Total 2 mL of the sample solution (Crude extract + Distilled water), 2 mL of Fehling′s solution A and B were added and boiled in a heated water bath. A red precipitate was formed which indicates the presence of reducing sugar.

Benedict's test for sugar (disaccharides)

Total 2 mL of the sample solution (Crude extract + Distilled water), an equal volume of benedict′s reagent was added to it. The mixture was heated on a boiling water bath for 2 min. The formation of reddish-brown precipitate confirms the presence of reduced sugar content.

Methylene Blue test for sugar (monosaccharides)

Total 3 mL of distilled water was taken in a test tube. To it a drop of 1% methylene blue and a few drops of 40% NaOH solution was added. The mixture was heated on a boiling water bath for 2 min and to it few drops of sample was added. The decolourisation of the blue colour indicated the presence of glucose or fructose in the sample.

Iodine test for starch (polysaccharides)

A few drops of the sample solution were taken in a test tube, to which a few drops of iodine solution were added. The mixture was heated in a boiling water bath for 2 minutes. The appearance of a dark blue colour indicated the presence of starch.

Biuret test for protein and amino acids

Total 2 mL of sample solution (sample + Distilled water), equal volume of biuret reagent is added. The appearance of violet colour specified the presence of protein.

Millon's test for protein and amino acids

Total 2 mL of the sample solution (Sample + Distilled water), 2 drops of Millon′s reagent were added and heated gently. A reddish-brown colouration was formed, which indicates the presence of proteins.

Xanthoproteic test for protein and amino acids

Total 2 mL of sample solution (sample + Distilled water), a small amount of concentrated nitric acid (NHO3) was added and the mixture was heated on a boiling water bath for 2 minutes. Then 1 mL of concentrated NH_4OH was added to the mixture. The formation of orange colour precipitate indicated the presence of protein.

Solubility test for Lipids

Four test tubes were taken and 3 mL of the sample solution (sample + Distilled water) was added to each test tube and marked as A, B, C, and D. To test tube A, water was added and mixed well. The presence of oily droplets indicated the presence of lipid. To test tube B, ether was added and mixed well. A homogeneous mixture was formed, indicating the presence of lipid. To test tube C, chloroform was added and mixed well. A homogeneous mixture was formed, indicating the presence of lipid. To test tube D, alcohol was added and mixed well. The formation of a precipitate at the bottom, which dissolved upon heating, indicated the presence of lipid.

Acrolein test for Lipids

Total 1 mL of sample solution (Sample + Distilled water), a few crystals of potassium metabisulphite were added. The mixture was then warmed in a hot water bath for 1minute. The appearance of pungent irritating smell of acrolein indicates the presence of lipids.

A heatmap illustrating the phytochemical profile of the methanolic extract of CR has been generated based on triplicate experimental observations. In this analysis, each phytochemical test was carried out following standard protocols and the optical density (OD) of the resulting reaction products was measured using a UV-visible spectrophotometer within the wavelength range of 400-770 nm, with distilled water serving as the blank control. These OD readings, reflecting the relative concentration or intensity of each phytochemical reaction, were recorded for all replicates and subsequently used to construct the heatmap. The visual representation provides a comparative overview of the phytochemical constituents present in the extract, emphasizing both consistency and variation across the triplicates.

Table 1 — HPTLC analysis of *C. rotundus* rhizome extract for phytoconstituent profiling and Rf value evaluation

Photo-plate	Mobile phase	Ratio	Number of spot visible	Spot intensity (visual)	Rf value (mean)
A	Chloroform (100%)	-	6	+++	0.725, 0.610, 0.580, 0.535, 0.335 and 0.200
B	Chloroform-Methanol	9:1	5	++	0.71, 0.625, 0.545, 0.36 and 0.220
C	Chloroform-Methanol	8:2	4	+	0.725, 0.455, 0.250 and 0.140

HPTLC: High-Performance Thin-Layer Chromatography, (+++): Strong spot (band) intensity, (++): moderate and (+): weak.

High-Performance Thin-Layer Chromatography (HPTLC) fingerprinting

HPTLC is commonly used to produce a plants chemical fingerprint to identify and quantify the main constituents within the plant[21]. The CR rhizome extract was applied on pre-coated silica gel on aluminium plate (Merck, Silica gel 60 F_{254}), previously activated at 105 °C for 2 hours. The mobile phase solvent system was developed with Chloroform, methanol and distilled water in the proportions as given in Table (1). The retardation factors (Rf) of all separated components were calculated.

Experimental design and animals

Swiss-Albino mice, weighing 20-25 grams, were purchased from the Animal House at the University of Science and Technology (USTM), Meghalaya, India. The mice were housed in cages lined with husk bedding and kept under controlled environmental conditions, including a temperature of 20±2°C, relative humidity of 60-70%, and a 12-hour light/dark cycle. They were provided with unlimited access to standard rat feed and water. Before conducting experiments, the mice were fasted overnight but had free access to water.

Cell line culture

Dalton′s Lymphoma ascites (DL) cells were gifted by Professor Surya Bali Prasad, Zoology department, NEHU and were inoculated and maintained in the laboratory mice. On the day of experiment, DL cells were collected from the tumor bearing mice, washed in 1× Phosphate Buffer Saline (PBS) and diluted to 1×10^6 cells/mL.

Dose selection

A single dose of the rhizome extract (200 µg/mL) was used to treat the DL cells and cisplatin (10 µg/mL) was taken as a standard reference drug[17].

Short term cytotoxicity assessment by Trypan blue exclusion assay

Cytotoxicity is typically represented as the percentage of dead cells in the population. The cytotoxicity effect of CR rhizome methanolic crude extract against DL cell lines was estimated by Trypan blue exclusion assay[22-24]. Stock cell suspension at a density of 1×10^6 was made in PBS, from which 300 µL of suspension was taken in 24 well plate as shown in the Fig. 2. The cells were treated with a single dose of 200 µg/mL CR extract for different hours (3, 6, 12 and 24 hours). Cisplatin (10 µg/mL) treated group was taken as positive control. Cells without treatment (PBS) was considered as normal control. From each well at different intervals, treated samples were collected and washed in PBS (pH 7.4). The cells were first exposed to a 1:1 (v/v) mixture of 0.4% Trypan blue dye and gently mixed on a slide. The slide was then examined under a microscope to count the total number of viable (unstained cells) and non-viable cells (blue stained cells) and cell viability was calculated accordingly. For quantification, ten microscopic fields were analysed per sample, with data derived from a total count of 1,000 cells. After counting the percentage viability was calculated as follows

$$\%\ \text{Cytotoxicity} = \frac{\text{Number of non} - \text{viable}}{\text{Total number of cells}} \times 100$$

Cell morphology study by Eosin staining technique

The cellular morphological changes were examined using eosin, an orange/red dye that binds to the basic cell structure[25]. Eosin is widely used histological technique in microscopy for visualising cellular structure and tissues. In this experiment, DL cells were treated with the same concentration (200 µg/mL) of *C. rotundus* crude extract and for identical time intervals as used in the Trypan blue exclusion assay. Cisplatin (10 µg/mL) was used as the positive control while untreated cells served as the normal control. At different time interval, treated samples were collected, washed in PBS (pH 7.4) and stained with eosin for 3 minutes. The slides were then examined under a microscope to identify morphological features indicative of apoptotic cell death. For quantification, ten microscopic fields were analysed per sample, and the data were compiled from a total of 1,000 cells counted.

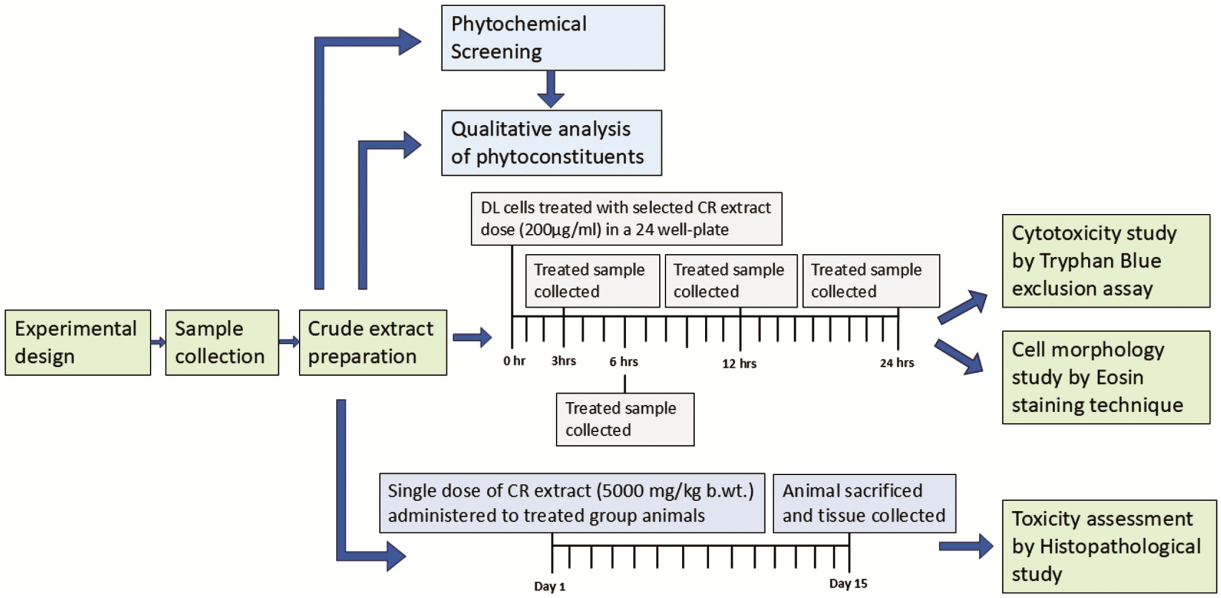

Fig. 2 — Schematic overview of the experimental design for phytochemical screening, cytotoxicity analysis and toxicity assessment in mice models.

Toxicity assessment of CR crude extract in mouse model

Preliminary toxicity studies were conducted to evaluate the toxic effects of CR rhizome crude extract on a murine model over a 14-day period, using a single high dose treatment of 5000 mg/kg body weight[26]. Two groups were formed: a control group and a treated group, each consisting of five healthy mice with an equal number of both sexes. A single dose of CR rhizome extract of 5000 mg/kg bw was administrated orally to the treated group while, the control group was administrated an equivalent volume (0.25 mL) of distilled water. The use of a single high dose of 5000 mg/kg bw was selected in accordance with internationally recognised guidelines for acute oral toxicity studies, particularly OECD Test Guideline 423.

The activity of the mice was regularly monitored for 14 days. The temperature was maintained within the range of 25-28 ºC with a 12-hour day and night cycle. The groups were regularly monitored to observe and identify behavioural changes and mortality during the period. After the completion of the period, the animals were sacrificed and some of the vital organs such as heart, lungs, spleen, liver, kidney, testis and ovary were grossly examined.

Statistical analysis

The results were presented as Mean ± S.D. and run in triplicates. The statistical significance of the treated groups at different time interval were evaluated by two-way ANOVA followed by Bonferroni post-hoc test for multiple comparisons. The value of P less than 0.05 were considered to be significant. All statistical analysis were performed using GraphPad Prism version 9.0 software.

Results

The phytochemical screening showed the presence of phytoconstituents in various degrees as depicted in the heat map (Fig. 3). The methanolic rhizome extract showed positive results for carbohydrate, sugars (Mono and disaccharides), protein and amino acids, alkaloids, glycosides, phenols, tannins, polyphenols, flavonoids, triterpenoids and lipids as measured by different test procedures. The heatmap (Fig. 3) illustrates the phytochemical profile of *C. rotundus* methanolic extract based on triplicate analysis (A, B and C). High and consistent optical density (OD) values were observed for carbohydrates (Fehling′s, Benedict′s and Molisch′s tests), glycosides, flavonoids, gums and mucilage and saponins, indicating their strong and reproducible presence across replicates. In contrast, alkaloids (Mayer′s and Wagner′s tests) exhibited consistently low OD values, suggesting poor presence in the extract. Proteins, phenols, tannins, polyphenols, and steroids showed moderate OD values with some variability across replicates. Overall, the analysis confirms that *C. rotundus* methanolic extract is rich in carbohydrates, glycosides, flavonoids, and mucilage, while alkaloid content is minimal.

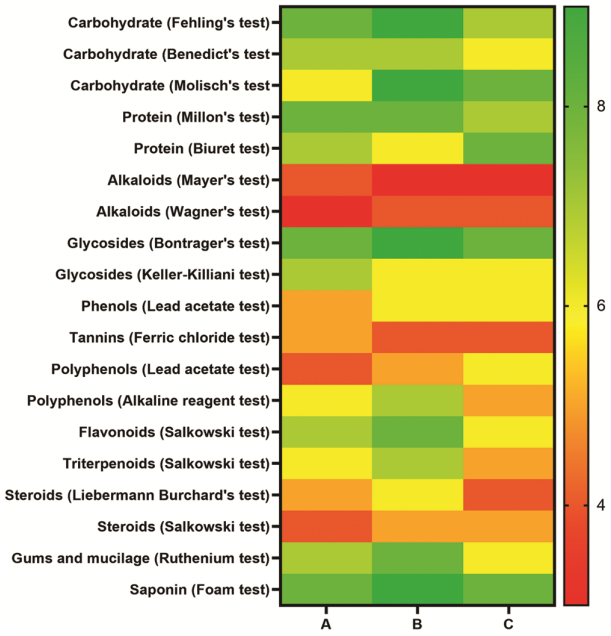

Fig. 3 — Heatmap analysis of phytochemical profiles in *Cyperus rotundus* methanolic extract. For heatmap analysis, the optical density (OD) of each reaction mixture was quantified spectrophotometrically (wavelength: 400-770), using water as blank. The recorded OD values were subsequently used to generate the heatmap.

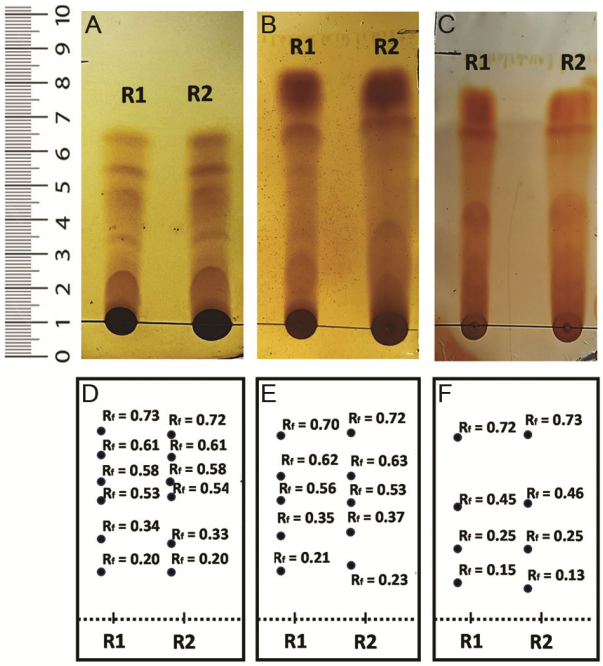

Fig. 4 — High-Performance Thin-Layer Chromatography (HPTLC) profiling of *Cyperus rotundus* crude extract with different mobile phase ratios: (A) Chloroform (100%), (B) Chloroform (9:1) and (C) Chloroform (8:2); (R1- Replica 1, R2- Replica 2). (a) represents the details of Rf values of (A), (b) represents the Rf values of (B) and (c) represents the Rf values of (C).

HPTLC fingerprinting profile

High-Performance Thin-Layer Chromatography (HPTLC) profiling of *CR* methanolic extract was carried out using three different mobile phase systems to assess its phytochemical composition. (Fig. 4 & Table 1) The chromatographic plates (A, B and C), run in two replicates (R1 and R2), exhibited consistent and reproducible banding patterns. Plate A, developed with 100% chloroform, showed six distinct spots with Rf values ranging from 0.20 to 0.725, indicating the presence of a wide range of non-polar phytochemicals. Plate B, using chloroform:methanol in a 9:1 ratio, revealed five spots with Rf values from 0.22 to 0.71, suggesting moderate polarity compounds and a slight shift in compound mobility due to the presence of methanol. Plate C, with a more polar mobile phase of chloroform:methanol (8:2), displayed four distinct spots with Rf values between 0.14 and 0.725, highlighting the presence of more polar constituents and reduced separation under these conditions. The consistent number and position of bands across replicates confirm the reproducibility of the method and indicate that solvent polarity plays a crucial role in the resolution and detection of phytochemical components in the extract.

Cytotoxicity assessment using Trypan blue exclusion assay

To assess the cell viability of DL cells following a single dose treatment with CR rhizome crude extract, a Trypan blue assay was performed. In this assay, the viable cells exhibit clear cytoplasm, while the non-viable cells appear blue in colour (Fig. 5). The results of the present study showed that a single dose (200 µg/mL) of the rhizome extract exhibited varying cytotoxic effects across different time intervals (3, 6, 12, and 24 hours). The viability of DL cells was found to be decreased at increasing time intervals. The graph (Fig. 6) depicted the time-dependent cytotoxic effect of *C. rotundus* (CR) extract (200 µg/mL) in comparison to cisplatin (10 µg/mL). At all time points, cisplatin induced significantly higher cytotoxicity than the CR extract, with differences reaching statistical significance at 3 hours ($*P < 0.05$), and at 6, 12 and 24 hours ($**P < 0.01$). Within the CR-treated group, cytotoxicity increased progressively over time. Significant differences were observed between 3 and 6 hours ($*P < 0.05$), 3 and 12 hours ($*P < 0.05$) and 3 and 24 hours ($***P < 0.01$). The most pronounced increase was detected between 3 and 24 hours ($***P < 0.001$), indicating a clear time-dependent cytotoxic response

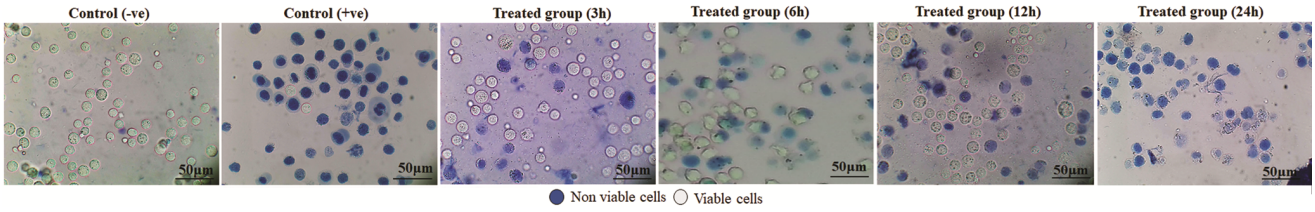

Fig. 5 — Photographs depicting the cytotoxic effects of a single dose of CR rhizome extract (200 µg/mL) in DL cells at various time intervals (3 h, 6 h, 12 h and 24 h) using trypan-blue exclusion assay.

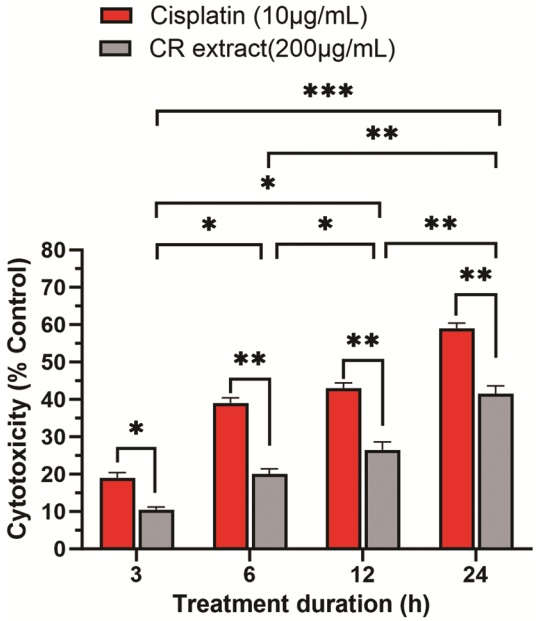

Fig. 6 — Cytotoxicity study of *Cyperus rotundus* (CR) rhizome crude extract (CE) at different time points assessed by Trypan blue exclusion assay. Cisplatin has been used as a positive control in this study. Data are presented as mean ± SD. Statistical significance was determined by two-way ANOVA. ***$P < 0.001$, **$P < 0.01$, *$P < 0.05$.

to CR extract, although its effect remained consistently lower than that of cisplatin throughout the treatment duration. Based on the viability, the median lethal time (LT_{50}) was estimated to be approximately 16.8 hours, further highlighting the time-dependent efficacy of the extract.

Cell morphology study

Eosin staining plays a critical role in evaluating cell morphology and detecting pathological alterations in various tissues. By enhancing the visibility of cell boundaries and cellular morphology, eosin effectively highlights the cytoplasm of cells, facilitating detailed observation. In the current study, the same concentration of CR rhizome extract (200 µg/mL) was utilised to assess cell morphology. The findings revealed significant morphological changes, including membrane blebbing, the formation of apoptotic bodies and protrusions or bulges on the cell surface as shown in the Fig. 7. The graph (Fig. 8) depicted the time-dependent induction of apoptosis by *C. rotundus* (CR) rhizome crude extract (200 µg/mL), compared with cisplatin (10 µg/mL), using morphological criteria (membrane blebbing, cytoplasmic vacuolation and membrane rupture). At 3 hours, both CR extract and cisplatin showed minimal apoptotic response with no statistically significant difference (ns). However, from 6 hours onward, cisplatin induced a significantly higher level of apoptosis compared to the CR extract (**$P < 0.01$). Within the CR-treated group, no significant (ns) difference was found between 3 and 6 hours. A significant increase in apoptosis was observed between 6 and 12 hours (*$P < 0.05$) and this trend continued between 12 and 24 hours (*$P < 0.05$). Additional comparisons within the CR group revealed significant differences between 3 and 12 hours (*$P < 0.05$) and between 6 and 24 hours (**$P < 0.01$), with the highest level of significant differences observed between 3 and 24 hours (***$P < 0.001$). These findings indicate a time-dependent increase in apoptosis induced by CR extract, although consistently lower than that of cisplatin.

Toxicity assessment

The rhizome extract of CR has demonstrated significant effects on the histological structure of various organs, including the liver, lungs, kidneys, heart, ovaries, testes, and spleen. The findings suggested that CR rhizome extract may have broad-spectrum protective and restorative effects on vital organ tissues, contributing to its potential therapeutic applications. The lack of notable differences between the control and treated groups underscores CR safety profile and its ability to preserve normal tissue integrity under experimental conditions. This suggests that CR can provide cytoprotective benefits without inducing adverse histological changes, further supporting its promise in clinical applications.

Histopathological study of heart

Histological study of the heart tissue exhibited a normal histological architecture in the control group

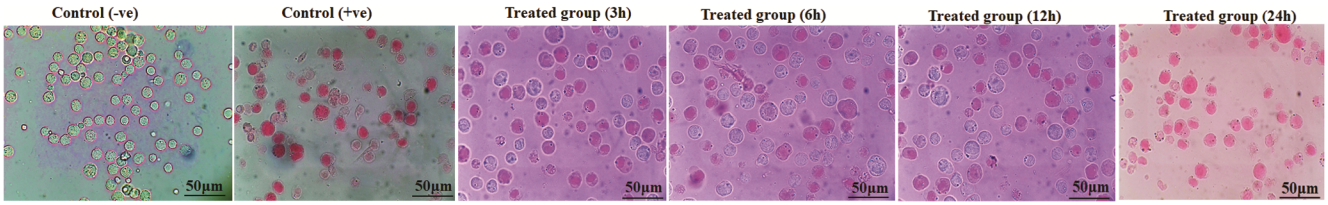

Fig. 7 — Photographs illustrating the morphological effects of a single dose of CR rhizome crude extract (200 µg/mL) in DL cells at different time intervals (3 h, 6 h, 12 h and 24 h) using eosin staining technique.

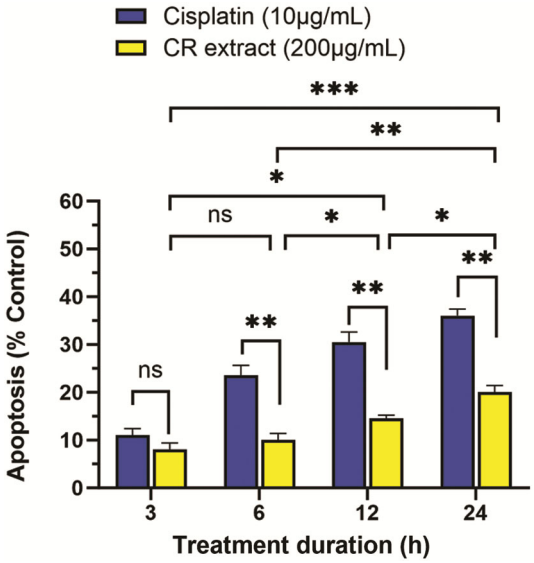

Fig. 8 — Apoptosis (membrane blebbing + cytoplasmic vacuoles + membrane rupture) induced by *Cyperus rotundus* (CR) rhizome crude extract (CE) at different time points assessed by Eosin staining method. Cisplatin has been used as a positive control in this study. Data are presented as mean ± SD. Statistical significance was determined by two-way ANOVA. ***$P < 0.001$, **$P < 0.01$, *$P < 0.05$. ns: non-significant.

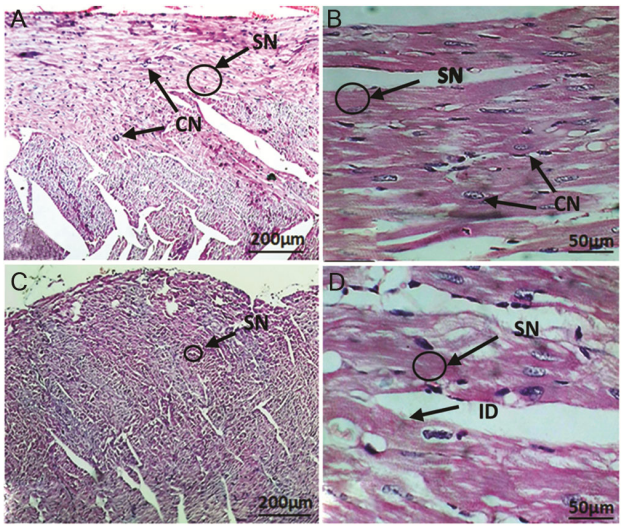

Fig. 9 — A comparative histological analysis of heart tissue sections from the control group [A (10x magnification) and B (40x magnification)] and the CR rhizome crude extract-treated group [C (10x magnification) and D (40x magnification)] showed normal architecture with clear striation (SN), normal central nuclei (CN) and prominent intercalated disc (ID) in both control and treated groups.

(Fig. 9). Cardiomyocytes were arranged in a regular pattern, with clear striations along with centrally located nuclei. Intercalated discs were prominent and uniformly distributed. The branched network of myocardial fibers were intact and exhibited no signs of degeneration or necrosis. Also, in the treated group, this structure appeared to be similar as the control group with no signs of degeneration or necrosis.

Histopathological study of lung

The histological structure of the lung tissue in control group showed normal architecture (Fig. 10). Alveoli were well-formed and evenly distributed, with clear and thin alveolar walls. Bronchioles lacking cartilage in their wall, allowing them to be more flexible and surrounding smooth muscle appeared normal, with no signs of structural alteration. There were no evidence of inflammation, fibrosis, or other pathological changes. Blood vessels were also intact and free from congestion or haemorrhage. In treated group, alveoli, alveolar walls, bronchioles, blood vessels appeared similar in structure as that of control with no sign of significant changes.

Histopathological study of liver

The histological structure of the liver tissue of control group maintained a normal morphological arrangement (Fig. 11). Hepatocytes were arranged in a characteristic trabecular pattern or in row, radiating from the central vein. Sinusoids remained clear and the portal triads were intact without any signs of pathological changes. Sinusoids were uniformly distributed between hepatocytes, with no signs of congestion or dilation. In treated group, hepatocytes, central vein, sinusoids appeared clear and normal with no abnormalities such as necrosis, inflammation, or fibrosis were observed, indicating that CR rhizome extract treatment does not induce any noticeable histopathological changes in liver tissue.

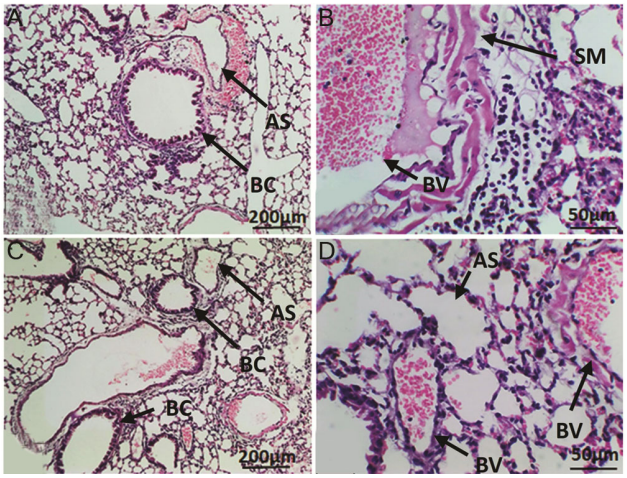

Fig. 10 — A comparative histological analysis of lung tissue sections from the control group [A (10x magnification) and B (40x magnification)] and the CR rhizome crude extract-treated group [C (10x magnification) and D (40x magnification)] showed normal structure of alveolus (AS), bronchioles (BC), blood vessel (BV) surrounded by smooth muscle (SM).

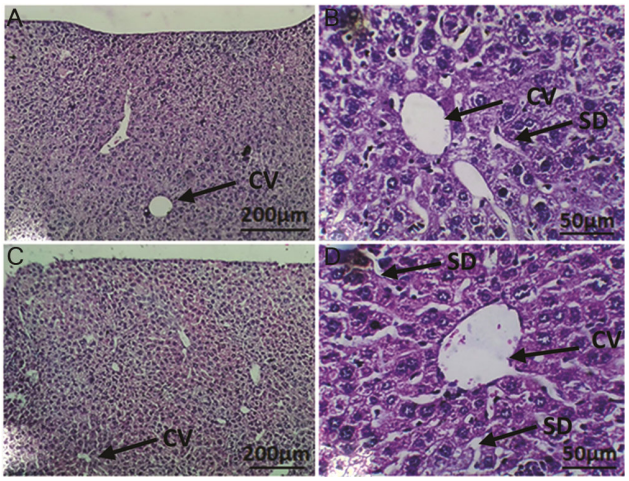

Fig. 11 — A comparative histological analysis of liver tissue sections from the control group [A (10x magnification) and B (40x magnification)] and the CR rhizome crude extract-treated group [C (10x magnification) and D (40x magnification)] showed normal architecture. Hepatocyte (HC) were arranged in row, radiating from central vein (CV); Sinusoids (SD) appeared normal between the hepatocyte plates in both control and treated groups.

Histopathological study of spleen

The spleen tissue maintained a normal histological appearance in both control and treated group (Fig. 12). In control group, the thick, densely stained outer layer known as capsule of the spleen was intact. Trabeculae extending from the capsule into the spleen′s interior were well-preserved, dividing the spleen into sections with no sign of morphological damages. The white pulp areas stained dark purple

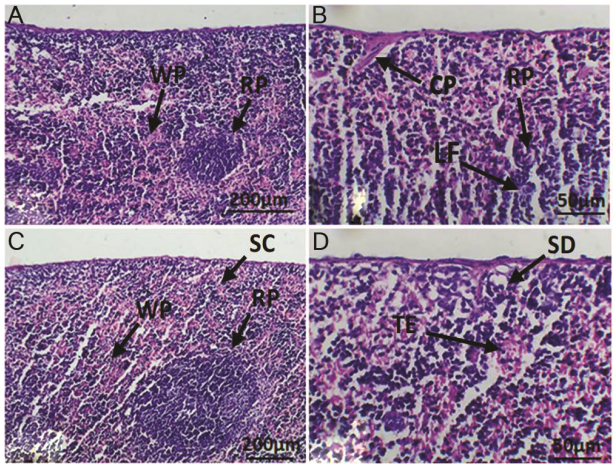

Fig. 12 — A comparative histological analysis of spleen tissue sections from the control group [A (10x magnification) and B (40x magnification)] and the CR rhizome crude extract-treated group [C (10x magnification) and D (40x magnification)] showed normal splenic tissue structure surrounded by capsule (CP) with clear differentiation between the white pulp (WP) and red pulp (RP) region. The trabeculae (TE), lymphoid follicles (LF), splenic cords (SC) and sinusoids (SD) exhibited no significant changes in the treated group maintaining similarity with the control group.

with H&E staining with high concentration of well-defined lymphoid follicles. The remaining lighter pink to red coloured regions represented the red pulp. These areas were organised into splenic cords and sinusoids. In treated group, the capsule, trabeculae, white pulp and red pulp maintained a normal and well-preserved structure, similar to that of the control group.

Histopathological study of kidney

The kidney tissue of the control animals exhibited normal histological architecture (Fig. 13). The renal cortex displayed well-defined dense and cluster glomeruli with clear Bowman's spaces and intact capillary tufts supported by fine connective tissue. The renal tubules, including proximal convoluted tubules displayed a well-developed brush border along with the presence of three to four nuclei with no signs of degeneration or necrosis. The distal convoluted tubules appeared smaller with a clearer lumen, containing five to six nuclei and lacking a brush border. The interstitial spaces were minimal, with no evidence of inflammation and pathological changes. In the treated group, there were no significant changes observed in the structure of glomerular capsule, proximal convoluted tubules, distal convoluted tubules and the interstitial spaces as compared to the control group.

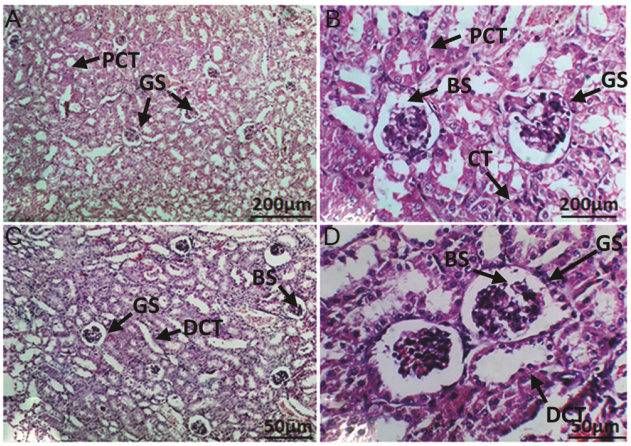

Fig. 13 — A comparative histological analysis of kidney cortex tissue sections from the control group [A (10x magnification) and B (40x magnification)] and the CR rhizome crude extract-treated group [C (10x magnification) and D (40x magnification)] showed normal renal architecture. The renal cortex in the control group exhibited well-defined, dense glomeruli (GS) with clear Bowman's spaces (BS) and intact capillary tufts (CT) supported by fine connective tissue. The proximal convoluted tubules (PCT) and distal convoluted tubules (DCT) appeared normal. In treated group, there were no such significant changes observed in the structures. No sign of degeneration, inflammation and fibrosis observed in the treated group.

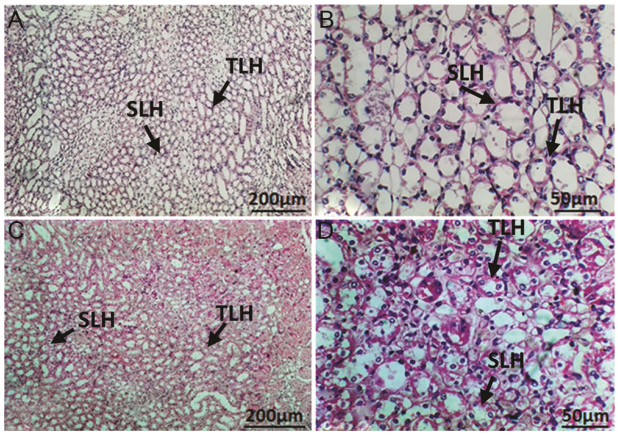

Fig. 14 — A comparative histological analysis of kidney medulla tissue sections from the control group [A (10x magnification) and B (40x magnification)] and the CR rhizome crude extract-treated group [C (10x magnification) and D (40x magnification)] showed sections of thin segments of loop of Henle (TLH) with thin-walled narrow tubes and lightly stained structures. The straight (ascending) segment of the distal tubule (SDT) appeared prominent with 9-10 nuclei. In treated group, there were no such structural changes in the loop of Henle, straight (ascending) segment of distal tubule and interstitial spaces compared to the control group. No sign of degeneration or necrosis were observed in the treated group.

The renal medulla displayed loops of Henle having thin-walled, narrow tubes, lightly stained circular structure (Fig. 14). Straight (ascending) segment of the distal tubule was prominent with smaller and narrower lumen containing 9 to 10 nuclei with less uniformly arranged convoluted cells. Thin segments of the loop of Henle containing 3 nuclei exhibited normal structural integrity. Collecting ducts were normal in appearance with large, well-defined lumen and thicker walls often clustered together with no signs of degeneration or necrosis. In addition, the treated group did not show any noticeable changes in the structure of the loops of Henle or the ascending segment of the distal tubule. The interstitial spaces also appeared similar to those in the control group.

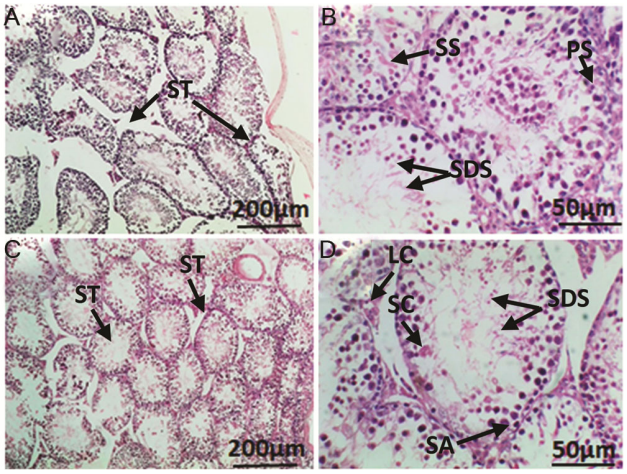

Fig. 15 — A comparative histological analysis of testis tissue sections from the control group [A (10x magnification) and B (40x magnification)] and the CR rhizome crude extract-treated group [C (10x magnification) and D (40x magnification)] showed normal histological structure with densely packed, rounded seminiferous tubules (ST) having clear lumen with developing sperm cells and an intact basement membrane. The germinal epithelium exhibited normal spermatogenic stages including spermatogonia (SA), primary (PS) and secondary spermatocytes (SS) and spermatids (SDS) supported by normal Sertoli cells (SC). The interstitial tissue containing Leydig cells (LC) were intact. In the treated group, no pathological changes were observed in the seminiferous tubules, germinal epithelium, spermatogenic stages, Leydig cells and Sertoli cells which displayed structural similarities to the control.

Histopathological study of testis

The histopathological study of testis tissue of the control animals exhibited normal histological structure (Fig. 15). Rounded densely packed seminiferous tubules were well-formed and evenly distributed, with a clear lumen filled with developing sperm cells and intact basement membrane. The germinal epithelium displayed normal spermatogenic stages, including spermatogonia, primary and secondary spermatocytes and spermatids. Sertoli cells were present and appear normal supporting the spermatogenic cells. The interstitial tissue containing

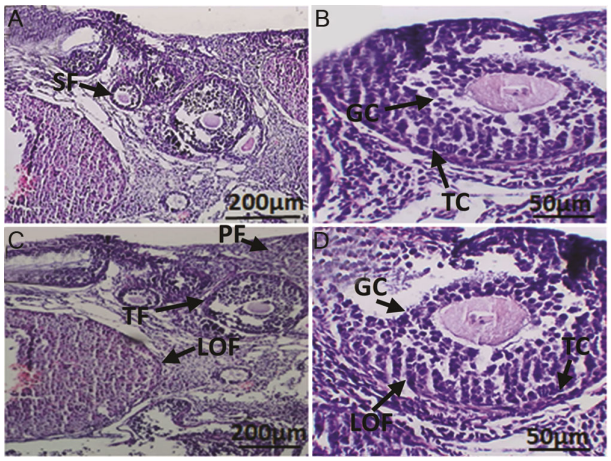

Fig. 16 — A comparative histological analysis of ovary tissue sections from the control group [A (10x magnification) and B (40x magnification)] and the CR rhizome crude extract-treated group [C (10x magnification) and D (40x magnification)] revealed normal architecture with intact germinal epithelium (GE) supported by a well-defined tunica albuginea. Large ovarian follicles (LOF) are well-preserved, showing clear distinctions between primary (PF), secondary (SF) and tertiary follicles (TF). The theca (TC) and granulosa cells (GC) surrounding the oocytes appear normal. In the treated group, the ovarian structure remained comparable to the control group, with intact germinal epithelium, tunica albuginea, and cortical follicles and no evidence of degeneration, fibrosis, or inflammation.

Leydig cells were intact. In treated groups, there were no signs of pathological changes in the structure of seminiferous tubules, germinal epithelium, spermatogonia, primary and secondary spermatocytes and spermatids. Sertoli cells and Leydig cells in the treated groups exhibited structural similarities to those in the control group.

Histopathological study of ovary

The histopathological study of the ovary in the control group displayed normal architecture. The germinal epithelium was intact, supported by well-defined tunica albuginea (Fig. 16). Ovarian follicles were well-preserved with clear distinctions among primordial, primary, secondary and tertiary follicles. Theca cells and granulosa cells surrounding the oocytes were normal. In the treated group, the ovarian structure was comparable to that of the control group, with no significant alterations observed. The germinal epithelium, tunica albuginea, cortical follicles were structurally intact with no signs of degeneration, fibrosis or inflammation.

Discussion

The present study conducted qualitative phytochemical screening and characterized the HPTLC profiles of the methanolic rhizome crude extract of CR. Additionally, the *in vitro* cytotoxic potential of the extract was evaluated against Dalton′s Lymphoma (DL) cells, along with an assessment of its toxicity in a murine model. The qualitative phytochemical analysis revealed that the plant is rich in primary and secondary metabolites such as carbohydrates, sugars (mono- and disaccharides), proteins and amino acids, and lipids, consistent with the findings of Samra *et al.,* where such metabolites were linked to pharmacological properties such as antioxidant and cytotoxic activities[27]. These constituents serve as precursors or structural components of bioactive compounds involved in various biological responses.

Further HPTLC profiling has revealed multiple well-resolved bands at distinct Rf values, indicating the presence of diverse phytoconstituents. The phytochemicals present in CR are known to possess a broad spectrum of pharmacological properties including anticancer, anti-inflammatory, anti-ulcer, antibacterial, antihypertensive, antidepressant, antioxidant, antimicrobial properties, cardiovascular protection and antidiabetic effects, antimalarial as well as potential efficacy in treating Parkinson's disease as previously reported[28-30]. The presence of these phytochemicals in the methanol extract of CR underscores its richness in active compounds and supports its traditional use in treating various ailments.

The *in vitro* cytotoxic activity of the methanolic rhizome extract of CR was assessed using cell viability assays i.e., the trypan blue dye method and cell morphology study by Eosin staining technique. The results demonstrated a positive cytotoxic response against DL cells. The Trypan blue method specifically revealed an increase in non viable DL cells following treatment with the extract. This align with the findings of Kilani *et al.*; Mannarreddy *et al.* where the cytotoxic effects were observed to be significantly increase in a dose and time-dependent manner in human cancer cell lines[16,31]. Additionally, morphological observations such as extensive membrane blebbing, cell shrinkage, and membrane disintegration further confirmed the induction of cell death. Thus, the cytotoxic effects observed in the Trypan blue dye exclusion assay and the apoptotic features confirmed by eosin staining can be attributed to the action of these phytochemicals. The presence of bioactive constituents mainly, phenolic compounds,

flavonoids and other oxidative stress-inducing agents, commonly found in *C. rotundus*, are known to interfere with cancer cell proliferation and induce programmed cell death. Recent studies by Kooshkmeydani *et al.* also support the anticancer mechanisms of such phytochemicals through apoptosis, strengthening the present findings[32]. The observed apoptotic features in DL cells also suggest that the extract has the potential to induce apoptosis that indicate the potential of the extract as anticancer agent indicating its promise as an anticancer agent. This finding could pave the way for further exploration through *in vivo* studies to better understand its therapeutic efficacy.

Further, the histopathological changes in the liver, lungs, heart, kidneys, spleen, testis, and ovary were examined following a single dose of CR rhizome extract revealed no significant structural changes in these organs suggesting its overall safety for therapeutic use. The liver displayed normal hepatic architecture with intact hepatocytes, sinusoids, and central veins, and no signs of necrosis or inflammation. The lungs retained normal alveolar and bronchiolar structures without congestion or edema. The heart exhibited intact cardiac muscle fibers with normal striations and no degenerative changes. The kidneys showed well-preserved glomeruli, Bowman′s capsules, and renal tubules with no evidence of pathological alterations. The spleen maintained its structural integrity with normal white and red pulp regions. The testis exhibited normal seminiferous tubules with intact germinal epithelium and healthy Sertoli and Leydig cells, while the ovary retained its normal architecture with intact germinal epithelium, tunica albuginea, and well-preserved follicles at various developmental stages. These results are consistent with previous studies carried out by Nidugala *et.al.*[32], who also reported that CR extract did not cause significant histopathological alterations in various vital organs, further supporting its safety profile.

Conclusion

From the above study, it can be concluded that CR rhizome crude extract exhibits significant anticancer efficacy by inducing apoptosis and cytotoxicity in DL cells, with effects increasing over time. A single dose of 200 µg/mL caused notable apoptotic changes, including vacuolarization and membrane blebbing. Furthermore, acute oral toxicity evaluation revealed no significant in major organs, indicating the extract′s safety at the tested dose. These findings support CR extract's potential as a natural anticancer agent, though further research should focus on the detailed elucidation of the molecular mechanisms involved in its apoptotic activity, the identification and isolation of active compounds responsible for the cytotoxic effect, and the evaluation of its *in vivo* efficacy using tumor-bearing models. Additionally, determining the safe therapeutic dosage range through sub-chronic and chronic toxicity studies will be essential to support its advancement toward clinical application.

Ethical statement

All procedures involving animals were approved by the IAEC of Cotton University, with proposal number 16/IAEC/CU/05/11/2020. The study was conducted in compliance with the Committee for the Purpose of Control and Supervision of Experiments on Animals (CPCSEA) guidelines, ensuring humane treatment and minimising animal suffering.

Funding statement

We extend our heartfelt gratitude to the Department of Biotechnology (DBT), Government of India, for enabling the use of the Central Facility established through their generous support under the DBT Builder project (Grant No: BT/INF/22/SP45376/ 2022) at Cotton University, Assam, India.

Acknowledgements

We extend our heartfelt gratitude and thanks to Mahua for technical support for carrying out the wet lab experiment. Special thanks to Dr. Ruprekha Dutta, Department of Dravyaguna Vigyan, Government Ayurvedic College and Hospital, Guwahati, Assam, for her invaluable assistance in providing knowledge about the sample and facilitating sample collection. We sincerely thank the Department of Biotechnology (DBT), Government of India for providing access to the resources of the Central Facility created under ongoing DBT Builder project at Cotton University (Grant No: BT/INF/22/SP45 376/ 2022).

Conflict of interest

The authors declare no conflict of interest

References

1 Gilani AH. Trends in ethnopharmacology. *J. Ethnopharmacol*, 100 (2005) 43.

2 Kinghorn AD, Pan L, Fletcher JN & Chai H. The relevance of higher plants in lead compound discovery programs. *J Nat Prod*, 74 (2011) 1539.

3 Gülcin I. Antioxidant activity of food constituents: an overview. *Arch Toxicol*, 86 (2012) 345.

4 Peschel W, Sánchez-Rabaneda F, Diekmann W, Plescher A, Gartzía I, Jiménez D, Lamuela-Raventós R, Buxaderas S & Codina C. An industrial approach in the search of natural antioxidants from vegetable and fruit wastes. *Food Chem*, 97 (2006) 137.

5 Jayakar V, Lokapur V, Nityasree BR, Chalannavar RK, Lasrado LD & Shantaram M. Optimization and green synthesis of zinc oxide nanoparticle using *Garcinia cambogia* leaf and evaluation of their antioxidant and anticancer property in kidney cancer (A498) cell lines. *Biomedicine (Taipei)*, 41 (2021) 206.

6 Ratna MG & Bahri S. The compound of purple nutsedge (*Cyperus rotundus*) tuber from province of lampung is potential as anticancer agent on the T47D breast cancer cell. *In Health Science International Conference*, 1 (2022) 20.

7 Nidugala H, Prabhu A, Avadhani R & Ravishankar B. *In vitro* anticancer efficacy of *Cyperus rotundus* (L.) on breast adenocarcinoma cells via the induction of DNA fragmentation and apoptosis. *Biomedicine (Taipei)*, 43 (2023) 1198.

8 Wang F, Song X, Ma S, Liu C, Sun X, Wang X, Liu Z, Liang D & Yu Z. The treatment role of *Cyperus rotundus* L. to triple-negative breast cancer cells. *Biosci Rep*, 39 (2019) BSR20190502.

9 Singh G. *Cyperus rotundus*: A potential medicinal plant. *J Pharmacogn Phytochem*, 13 (2024) 27.

10 Singh N, Pandey BR, Verma P, Bhalla M & Gilca M. Phyto-pharmacotherapeutics of *Cyperus rotundus* Linn. (Motha): an overview. *Indian J Nat Prod Resour*, 3 (2012) 467.

11 Al-Snafi AE. A review on *Cyperus rotundus* A potential medicinal plant. *IOSR J Pharm*, 6 (2016) 32.

12 Bezerra JJ & Pinheiro AA. Traditional uses, phytochemistry, and anticancer potential of *Cyperus rotundus* L. (Cyperaceae): A systematic review. *S Afr J Bot*, 144 (2022) 175.

13 Sudirman S. Phytochemical and pharmacological study of teapot grass (*Cyperus rotundus* L) as a medicinal plant. *Hayyan J*, 1 (2024) 1.

14 Ounjaijean S, Lektip C & Somsak V. *In vivo* antimalarial activity of *Cyperus rotundus* and its combination with dihydroartemisinin against *Plasmodium berghei*. *Adv Pharmacol Pharm Sci*, 2024 (2024)1.

15 Soumaya KJ, Dhekra M, Fadwa C, Zied G, Ilef L, Kamel G & Leila CG. Pharmacological, antioxidant, genotoxic studies and modulation of rat splenocyte functions by *Cyperus rotundus* extracts. *BMC Complement Altern Med*, 13 (2013) 1.

16 Mannarreddy P, Denis M, Munireddy D, Pandurangan R, Thangavelu KP & Venkatesan K. Cytotoxic effect of *Cyperus rotundus* rhizome extract on human cancer cell lines. *Biomed Pharmacother*, 95 (2017) 1375.

17 Rajamohan S. Harbouring the potential of medicinal and aromatic plants of India: Novel biotechnological approach and extraction technologies. *M & APs, Cham: Springer International Publishing*, 1 (2022) 323.

18 Harborne JB. Phytochemical Methods: A Guide to Modern Techniques of Plant Analysis .1990, 115.

19 Kumari Sneha. Practical and viva community medicine. *Int J Hea Edu Med Inf*, 5 (2018) 24.

20 Verma S, Rani S, et al. Qualitative tests for preliminary phytochemical screening: An overview. *J Pharmacogn Phytochem*, 8 (2020) 248.

21 Jain, D, Upadhyay, R, Jain, S, Prakash, A & Dr. P TLC and HPTLC finger printing analysis of *Cyperus rotundus* (Linn.). *Lett Appl NanoBioScience*, 11 (2022) 3861.

22 Strober W. Trypan blue exclusion test of cell viability. *Curr Protoc Immunol*, 111 (2015) A3.

23 Kuttan R, Bhanumathy P, Nirmala K & George MC. Potential anticancer activity of turmeric (*Curcuma longa*). *Cancer Lett*, 29 (1985) 197.

24 Turkki R, Linder N, Kovanen PE, Pellinen T & Lundin J. Identification of immune cell infiltration in hematoxylin-eosin stained breast cancer samples: texture-based classification of tissue morphologies. *In Med Imag, Digi Pathol,* 9791 (2016) 273.

25 Fischer AH, Jacobson KA, Rose J, Zeller R. Hematoxylin and eosin staining of tissue and cell sections. *CSH Protoc,* 5 (2008) 4986.

26 S hanabhorn S, Jaijoy K, Thamaree S, Ingkaninan K & Panthong A. Acute and subacute toxicities of the ethanol extract from the rhizomes of *Cyperus rotundus* Linn. *Warasan Phesatchasat*, 32 (2005) 15.

27 Prakash, A., Jain, D., & Tripathi, R. Pracheta. Pharmacognostical analysis of different parts of *Cyperus rotundus* L. *Plant Sci Today* 6 (2019) 12.

28 Samra RM, Soliman AF, Zaki AA, Ashour A, Al-Karmalawy AA, Hassan MA & Zaghloul AM. Bioassay-guided isolation of a new cytotoxic ceramide from *Cyperus rotundus* L. *S Afr J Bot*, 13 (2021) 210.

29 Li AN, Li S, Zhang YJ, Xu XR, Chen YM & Li HB. Resources and biological activities of natural polyphenols. *Nutrients*, 6 (2014) 6020.

30 Taheri, Y., Herrera-Bravo, J., Huala, L., Salazar, L. A., Sharifi-Rad, J., Akram, M., Shahzad, K., Melgar-Lalanne, G., Baghalpour, N., Tamimi, K., Mahroo-Bakhtiyari, J., Kregiel, D., Dey, A., Kumar, M., Suleria, H. A. R., Cruz-Martins, N., & Cho, W. C. (2021). *Cyperus* spp.: A Review on Phytochemical Composition, Biological Activity, and Health-Promoting Effects. *Oxidative medicine and cellular longevity* (2021) 4014867.

31 Kilani S, Sghaier MB, Limem I, Bouhlel I, Boubaker J, Bhouri W, Skandrani I, Neffatti A, Ammar RB, Dijoux-Franca MG & Ghedira K. *In vitro* evaluation of antibacterial, antioxidant, cytotoxic and apoptotic activities of the tubers infusion and extracts of *Cyperus rotundus*. *Bioresour Technol*, 99 (2008) 9004.

32 Nidugala H, Avadhani R, Prabhu A & Ravishankar B. The toxicological and histopathological effects of aqueous and ethanolic extracts of *Cyperus rotundus* rhizomes in Ehrlich ascites carcinoma induced in Swiss albino mice. *J Anat Soc India*, 68 (2019) 99.